CrossMark
click for updates

View Article Online
View Journal

Dalton Transactions

Accepted Manuscript

This article can be cited before page numbers have been issued, to do this please use: K. Bamford, L. Longobardi, L. Liu, S. Grimme and D. W. Stephan, *Dalton Trans.*, 2017, DOI: 10.1039/C7DT01024A.

This is an Accepted Manuscript, which has been through the Royal Society of Chemistry peer review process and has been accepted for publication.

Accepted Manuscripts are published online shortly after acceptance, before technical editing, formatting and proof reading. Using this free service, authors can make their results available to the community, in citable form, before we publish the edited article. We will replace this Accepted Manuscript with the edited and formatted Advance Article as soon as it is available.

You can find more information about Accepted Manuscripts in the author guidelines.

Please note that technical editing may introduce minor changes to the text and/or graphics, which may alter content. The journal's standard Terms & Conditions and the ethical guidelines, outlined in our author and reviewer resource centre, still apply. In no event shall the Royal Society of Chemistry be held responsible for any errors or omissions in this Accepted Manuscript or any consequences arising from the use of any information it contains.

ROYAL SOCIETY OF CHEMISTRY

rsc.li/dalton

Please do not adjust margins
View Article Online
DOI: 10.1039/C7DT01024A

Dalton Transactions

Paper

Published on 28 March 2017. Downloaded by University of Newcastle on 28/03/2017 21:38:16.

FLP Reduction and Hydroborations of Phenanthrene *o*-Iminoquinones and α-Diimines†

Received 00th January 20xx,
Accepted 00th January 20xx

DOI: 10.1039/x0xx00000x

www.rsc.org/

Karlee L. Bamford,[a] Lauren E. Longobardi,[a] Lei Liu,[b] Stefan Grimme,[b] and Douglas W. Stephan[a]*

Redox active, or non-innocent, ligands containing O or N heteroatoms are frequently used in transition metal complexes, imparting unique catalytic properties, but have seen comparatively limited use in the chemistry of group 13 elements. In this article we report the frustrated Lewis pair (FLP) hydrogenations and hydroboration of an N-aryl-phenanthrene-*o*-iminoquinone and two N,N'-diaryl-phenanthrene α-diimines. These reactions exploit $B(C_6F_5)_3/H_2$, $HB(C_6F_5)_2$ and $H_2BC_6F_5{\cdot}SMe_2$ to give a series of derivatives including 1,3,2-oxaza- and diazaboroles and borocyclic radicals. The reaction pathways leading to these products are outlined and supported by DFT-calculations and experimental insight. The modular and unusual synthetic strategies described herein give access to new boroles as well as air-stable boron-containing radicals, thus extending the chemistry of redox active ligands in main group systems.

Introduction

The synthesis and isolation of stable radicals is an on-going challenge in main-group chemistry. This is motivated both by the fundamental interest in such open-shell species[1] and by the potential for embedding them within conjugated materials to access new optoelectronically active materials.[2-5] Examples of such materials featuring group 13 elements, particularly boron, have become more abundant in the literature in recent years. Stable boron-containing radicals have been made accessible through a variety of synthetic means, including the: i) reduction of boranes,[6] borane complexes,[7] diboranes,[8] and boroles[9] to give anionic radical species; ii) reduction of donor-stabilized borenium cations, to neutral boryl radicals;[10] and iii) oxidation of spiroborates to zwitterionic radicals.[11]

Examples of amine-ligated boron radicals are limited in number and variety, but have been prepared by the chemical reduction of base-stabilized boranes[12, 13] and from reactions of redox-active ligands with boranes.[14, 15] Early work in the former area revealed that without base-stabilization, reduction of organohaloboranes affords diamagnetic borolanylborolanes.[16] The reactions of the diaza-homologue of a semiquinone (*i.e.* a semidiimine) in anionic form with boron halides yields 1,3,2-diazaborocyclic radical (Chart 1, A) *via* salt metathesis.[14] While analogous salt metathesis approaches have been widely used in the preparation of transition metal complexes of polyaromatic semiiminoquinone and semidiimine ligands,[17-21] group 13 derivatives are few in number and are largely unknown for boron in particular.[22-24,25] Recent reactions of boranes and the redox-active ligand N,N'-1,4-diazabutadienes[26, 27] have targeted families of borocations although the corresponding neutral open-shell analogs have received limited attention.[15,28]

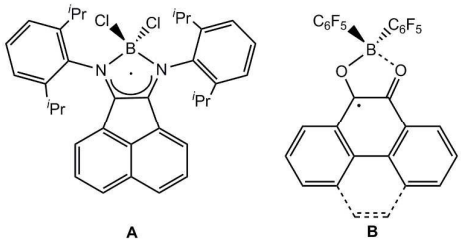

Chart 1. Examples of polyaromatic borocyclic radicals.

Our group has added a new frustrated Lewis pair (FLP) hydrogenation approach involving reactions of $B(C_6F_5)_3$, H_2 and polyaromatic diones to give remarkably air-stable, neutral 1,3,2-dioxoborocyclic radicals (Chart 1, B).[29] Most recently we have examined the reactivity of these radicals with a variety of nucleophiles affording a unique approach to a series of novel zwitterions with concurrent electron transfer reactions.[30] Herein we expand our approach, exploiting hydrogenation and hydroboration reactions of phenanthrene *o*-iminoquinones and α-diimines to generate a new air-stable 1,3,2-oxaza- and diazaboroles and borocyclic radicals.

Results and Discussion

An equimolar mixture of N-(2,6-dimethylphenyl)-phenanthren-*o*-iminoquinone (**1**) and $B(C_6F_5)_3$ in toluene was treated with H_2 (4 atm) in a J-young NMR tube and heated to 110 °C for 0.5 h

[a] *Department of Chemistry, University of Toronto, 80 St. George St., Toronto, Ontario M5S 3H6, Canada Email: dstephan@chem.utoronto.ca.*
[b] *Institut für Anorganische und Analytische Chemie, Westfälische Wilhelms-Universität Münster, Corrensstrasse 30, 48149 Münster Germany*

† Electronic Supplementary Information (ESI) available: Experimental details. Crystallographic Data was deposited (CCDC 1535312-1535321 See DOI: 10.1039/x0xx00000x

Dalton Transactions Accepted Manuscript

Please do not adjust margins

View Article Online
DOI: 10.1039/C7DT01024A

Published on 28 March 2017. Downloaded by University of Newcastle on 28/03/2017 21:38:16.

(Scheme 1), affording a dark brown solution. ^{19}F and ^{11}B NMR spectra of the reaction mixture confirmed consumption of $B(C_6F_5)_3$ The ^{19}F NMR signals showed three signals assigned to HC_6F_5, and five other resonances that were broad (w_b = 130 Hz) and one very broad signal at -159.9 ppm (w_b =1300 Hz) while a single ^{11}B NMR signal was observed at 10.4 ppm. These data are consistent with the formation of a new species **3** that exhibits some degree of inhibited rotation about the B–C bonds and a second product, **4**, that is likely paramagnetic.

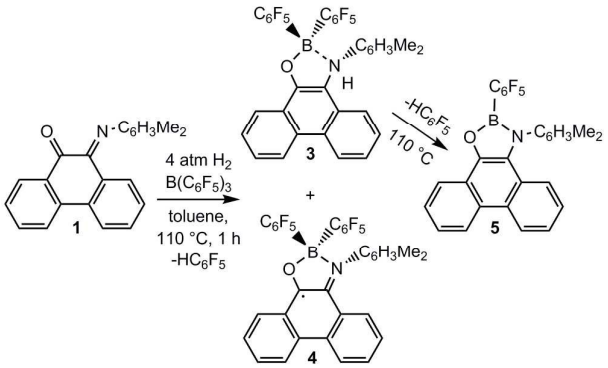

Scheme 1. Reaction of compound **1** and $B(C_6F_5)_3$ under 4 atm H_2 ($C_6H_3Me_2$ = 2,6-dimethylphenyl).

Fortuitously, a dilute pentane solution of the **3**/**4** mixture left to slowly evaporate furnished several bronze crystals that were shown by single crystal X-ray diffraction to be the amine-ligated borinic ester $C_{14}H_8O(NHC_6H_3Me_2)B(C_6F_5)_2$ **3** (

Figure **1**a). Compound **3** displays a pseudo-tetrahedral geometry about the boron atom, with O-B-C_6F_5 angles of 106.8(2)° and a B–N bond length of 1.706(6) Å.

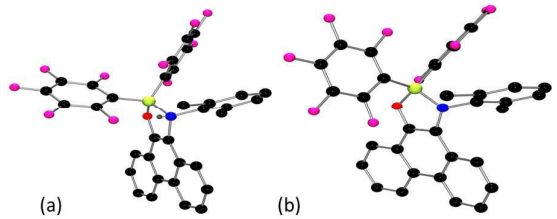

Figure 1. POV-ray depictions of (a) **3** and (b) **4**, with C–H atoms omitted for clarity. Atom colour scheme: H: grey; B: yellow-green; C: black; N: blue; O: red; F: pink.

Solutions of pure **4** are intensely brown in colour and UV-vis spectroscopic analysis revealed an absorption band at 423 nm having a molar absorptivity of 1.3 x 10^3 $L{\cdot}cm^{-1}{\cdot}mol^{-1}$ (see ESI). Compound **4** gives rise to a single broad ^{19}F NMR resonance (-159.9 ppm) but is otherwise NMR silent and exhibits an EPR signal (*vide infra)*. CH_2Cl_2 solutions of compound **4** cooled to -35 °C led to the isolation of black-brown crystals. The molecular structure (

Figure **1**b) verified the identity of **4** as the target 1,3,2-oxazaborocyclic radical, $[C_{14}H_8O(NC_6H_3Me_2)B(C_6F_5)_2]^{\bullet}$. The B–O bond distance is notably increased in **4** (1.514(4) Å) compared with **3** (1.478(5) Å), while the B–N bond distance is decreased to 1.601(5) Å *versus* 1.706(6) Å in **3** (Table 1). The (O)C–C(N) bond length for **4** (1.405(5) Å) lies between typical C–C and C=C bond lengths, while the dihedral angle between the 2,6-dimethylphenyl substituent on N and the plane of the oxazaborole is 77.7(3)°.

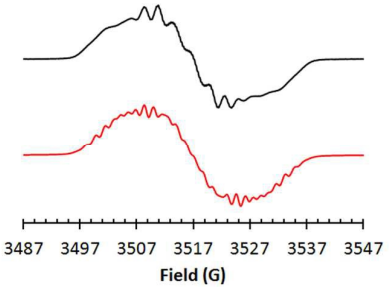

Figure 2. Experimental X-band EPR spectrum of **4** in toluene at 298 K (black: mod. amp. = 1) and simulated EPR spectrum (red line: g = 2.0039; $a(^{11}B)$ = 4.25 G, $a(^{14}N)$ = 5.17 G, $a(^{1}H)$ = 1.42-3.98 G (8H)).

EPR spectroscopic analysis of **4** (Figure 2) revealed coupling of the unpaired spin density to ^{14}N, ^{11}B, ^{19}F (10F) and ^{1}H (8H) nuclei. The complex fine-structure resulting from these couplings was not resolved and thus a range of fitted coupling constants gave good correlation between simulated and experimental spectra. Similar complications have been encountered for related group 13 element radicals. [13,32,33] The simulated spectrum presented herein was optimized from computed hyperfine coupling constants (PBE0/def2-QZVP//PBEh-3c, see ESI). Coupling to ^{1}H nuclei is consistent with delocalization of the unpaired spin density over the ligand framework. Computational models of the SOMO and spin-density distribution of **4** at multiple levels of theory (see Figure 3 and ESI) are also consistent with such delocalization. Qualitatively, these spectra are similar to those seen for the dioxoborocyclic radicals,[29] however the indicated LUMO and SOMO energies (-3.66 eV and -5.87 eV) for **4** are higher than those determined for the phenanthrene-based dioxoborocyclic radical (the energies of LUMO and SOMO are -4.323 eV and -6.550 eV, respectively)[29] by the PW6B95/def2-TZVP//PBEh-3c level. These differences are related to the electronegativity differences between oxygen and nitrogen, resulting in an overall lowering of all the molecular orbitals in the dioxo-radical species. Experimentally, the aromatic stabilization in **4** manifests as its remarkable stability in air.[34]

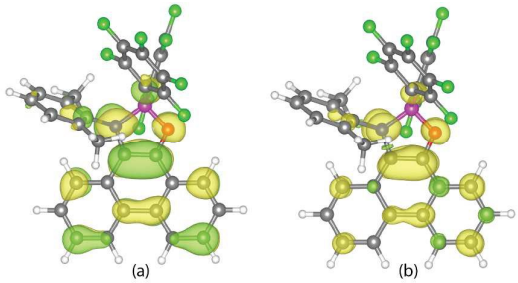

Figure 3. Calculated SOMO (a) and spin density (b) of compound **4**. Contour surface value: 0.03 a.u. and 0.002, respectively. Computational level: PW6B95/def2-TZVP//PBEh-3c. Atom colour scheme: H: white; B: pink; C: black; O: red; F: green.

Cyclic voltammetric studies of **4** (see ESI) using the ferrocene/ferrocenium couple (Fc/Fc^{+}) as the reference

Dalton Transactions Accepted Manuscript

This journal is © The Royal Society of Chemistry 20xx

Please do not adjust margins
View Article Online
DOI: 10.1039/C7DT01024A

Published on 28 March 2017. Downloaded by University of Newcastle on 28/03/2017 21:38:16.

revealed a pseudo-reversible wave centred at -0.63 V. This indicates that **4** is less easily reduced than its dioxo-homologues ($E_{½}$ = -0.27 V). This is consistent with the higher energy calculated for the SOMO, which suggests a lower electrophilicity than the the corresponding orbital in the dioxo-homologue.

Heating reaction mixtures of **1** and $B(C_6F_5)_3$ under H_2 in toluene for an additional 2.5 h at 110 °C did not change the dark appearance of the solution but led to complete consumption of **3** and the growth of *ortho*-, *para*-, and *meta*-C_6F_5 resonances attributable to a species **5** alongside those signals attributable to HC_6F_5 (see ESI). The corresponding ^{11}B NMR spectrum for **5** shows only a single broad resonance at 28.6 ppm. The spectroscopic data attributable to **5** are typical of 1,3,2-oxazaboroles, suggesting the formulation as $C_{14}H_8O(NC_6H_3Me_2)BC_6F_5$.[35,36] Nonetheless, the isolated solid proved to be a mechanical mixture of dark brown and white solids, both of which exhibited moderate-to-excellent solubility in common organic solvents, precluding facile separation. Flash chromatography and sublimation proved to be similarly ineffective. MS analysis of the crude mixture confirmed the presence of two species having mass-to-charge ratios consistent with the 1,3,2-oxazaborocyclic radical (**4**) and a 1,3,2-oxazaborole (**5**). Successive recrystalizations lead to the isolation of **4** in 34 % yield.

The challenge of isolating compound **5** cleanly from the initial hydrogenation reaction prompted efforts to uncover an alternative route. Treatment of **1** with one equivalent $H_2B(C_6F_5)\cdot SMe_2$ ("Lancaster's reagent")[37] in toluene afforded a clear and colourless solution within 1 h of mixing at ambient temperature (Scheme 2). ^{11}B and ^{19}F NMR spectra for this reaction indicated complete consumption of Lancaster's reagent after 2 h and clean formation of **5**, which could be isolated in 89% yield following purification by sublimation. X-ray diffraction quality single crystals of **5** were grown from CH_2Cl_2 at -35 °C. The structure of **5** (Figure 4) is similar to related 1,3,2-oxazaboroles with a five-membered O-B-N heterocycle that is not strictly planar as a result of the trigonal pyramidal geometry about N.[38] The cyclic voltammogram for **5** (see ESI) displays irreversible oxidations at E_{pa} values of 0.73 V and 1.41 V.

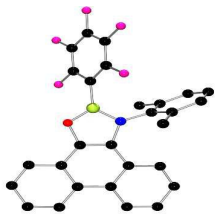

Figure 4. POV-ray depiction of **5**, with H atoms omitted for clarity. Atom colour scheme: B: yellow-green; C: black; N: blue; O: red; F: pink.

An alternative synthetic route to **4** was derived from the reaction of **1** with one equivalent of $HB(C_6F_5)_2$ ("Piers' borane") in toluene at ambient temperature. The immediately formed dark brown solution shows complete consumption of $HB(C_6F_5)_2$ and the formation of compounds **3** and **4** by ^{11}B and ^{19}F NMR spectroscopic analysis. After 3 h heating at 110 °C the conversion of **3** to **5**, accompanied by loss of HC_6F_5, was apparent (Scheme 2).

Table 1. Selected geometric parameters of compounds **3**-**5**. Computed values (PBEh-3c level) are given in parentheses for comparison.

compound	**3**	**4**	**5**
d[B–O] (Å)	1.478(5)	1.514(4)	1.383(3)
	(1.460)	(1.4964)	(1.376)
d[B–N] (Å)	1.706(6)	1.601(5)	1.415(3)
	(1.723)	(1.602)	(1.416)
d[(O)C-C(N)] (Å)	1.345(6)	1.405(5)	1.368(3)
	(1.325)	(1.409)	(1.361)
O–B–N (°)	100.9(3)	99.0(2)	109.5(2)
	(100.2)	(98.8)	(108.5)
O–B–C_6F_5 (°)	106.8(2)	110.1(2)	124.0
	(108.5)	(112.2)	(123.5)
N–B–C_6F_5 (°)	111.1(3)	108.4(2)	126.5
	(110.6)	(108.1)	(127.9)

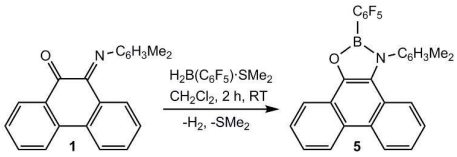

Scheme 2. Reaction of compound **1** and $H_2B(C_6F_5)\cdot SMe_2$ ($C_6H_3Me_2$ = 2,6-dimethylphenyl).

The mechanism of formation of **3**-**5** in the reaction of **1** with $B(C_6F_5)_3$ and H_2 was considered further. By analogy to the proposed mechanism for the formation of dioxoborocyclic radicals,[29] an amino-alcohol (**6**), resulting from $B(C_6F_5)_3$-mediated hydrogenation of **1**, is proposed to react with $B(C_6F_5)_3$ to give **3** and, subsequently, **5**. It is interesting to note that in the structure of **3**, the NH···C_6F_5(*ipso*) distance is 2.6594 Å), which is within the sum of the van der Waal radii (2.9 Å), foreshadows the protonation of the perfluorophenyl ring leading to elimination of HC_6F_5 en route to **5**.

A possible pathway to **4** was considered in which reduction of **1** to $C_{14}H_8OH(NHC_6H_3Me_2)$ (**6**) and subsequent conproportionation with **1** generated the neutral semiiminoquinone radical $[C_{14}H_8O(NHC_6H_3Me_2)]^{\bullet}$ (Scheme 3). To the best of our knowledge, the formation of such a *neutral* phenanthrene-based semiiminoquinone has not been reported, although the phenomenon has been documented for other *o*-iminoquinone derivatives.[39,40,41] To probe this possibility, **6** was independently prepared and structurally characterized (see ESI) by a Pd-catalyzed hydrogenation of **1**.[42] Treating **6** with one equivalent of **1** resulted in a mixture that was dark green in colour. The ^1H NMR spectrum of this mixture showed broadened methyl resonances from the N-bound substituent of **1** and **6** (see ESI), while the EPR spectrum and its DFT-supported simulation (see ESI) were consistent with the formation of free semiiminoquinone radical (**E**, Scheme 3). Although attempts to isolate the semiiminoquinone radical were unsuccessful, solutions of the *in-situ* generated semiiminoquinone treated with a stoichiometric amount of $B(C_6F_5)_3$ immediately turned from dark green to dark brown in colour, suggesting formation of **4**. Multinuclear NMR spectra were consistent with the formation of **3** and **4** and revealed

Dalton Transactions Accepted Manuscript

Please do not adjust margins

View Article Online
DOI: 10.1039/C7DT01024A

Published on 28 March 2017. Downloaded by University of Newcastle on 28/03/2017 21:38:16.

complete consumption of $B(C_6F_5)_3$ in 0.5 h at ambient temperature. Crucially, reaction of **6** with one equivalent of $B(C_6F_5)_3$ at room temperature yields only the intermediate **3**, as detected by DART-MS and ^{19}F NMR spectroscopy. Subsequent heating of the reaction mixture produced compound **5** and HC_6F_5. Most convincingly, the reaction mixtures before and after heating were found to be EPR silent. Thus the proposed mechanism for the formation of **3** and **5** (Scheme 3) resembles that proposed for the dioxoborocyclic radicals and is supported by the observation of key intermediates that evaded isolation for the dioxo-homologues.[29]

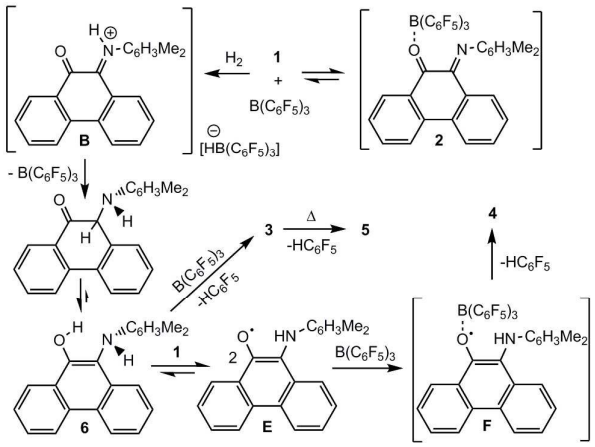

Scheme 3. Proposed mechanism for the formation of products **3**, **4,** and **5** ($C_6H_3Me_2$ = 2,6-dimethylphenyl).

DFT methods were used to compute the energy profiles for the investigated reactions. All structures were optimized with a composite DFT method PBEh-3c,[43] followed by single point energy calculations at the PW6B95-D3 level of theory[44-46] with a large Gaussian AO def2-TZVP basis set.[47, 48] The COSMO-RS (Conductor-like Screening Model for Real Solvents) solvation model[49, 50] (with toluene as the solvent) was used to compute solvation free energies (for computational details, see ESI). According to the DFT analysis, the reaction proceeds *via* an initial FLP cleavage of H_2 affording an ion-pair that ultimately generates **6**, which reacts competitively with $B(C_6F_5)_3$ or **1**. The kinetically-preferred latter pathway generates the semiiminoquinone radical **E** which reacts with $B(C_6F_5)_3$ to yield **4** (Scheme 3). The rate determining step in the formation of **4** is the elimination of HC_6F_5 from the $B(C_6F_5)_3$ adduct of the semiiminoquinone radical (**F**), with an energy barrier of 34.2 kcal·mol^{-1}. The thermodynamically favoured pathway produces **3**, which subsequently eliminates HC_6F_5 to give **5**. The energy barrier to the formation of **5** similarly involves the protonation of a perfluorophenyl ring and was computed to be 41.4 kcal·mol^{-1}. It is important to point out that the computed high energy barriers are qualitatively consistent with the experimental conditions. For example, the formation of **3** and **4** occurs at high temperature (110 °C) and the conversion of **3** to **5** requires an even higher temperature of 150 °C for a fixed reaction time of 0.5 h. However, on an absolute scale, the computed barriers seem inordinately high (about 5-10 kcal/mol). This may be explained by the errors arising from the treatment of solvation or by an energy offset (*i.e.* a systematic error) in the reference point for the zero of free energy.The reaction of Piers' borane and **1** was also considered computationally. Pathways involving 1,2- and 1,4-hydroborations affording the α-boryloxy imine (**K**) and **3** were computed. While the products **K** and **3** are formed from **1** with small barriers of 5.3 and 6.4 kcal·mol^{-1}, respectively, the barrier to the imine-enamine tautomerism was found to be 29.3 kcal·mol^{-1}. Oxidation of **K** by **1** to give **E** and **4** is computed to proceed with a remarkably-low activation barrier of 6.0 kcal·mol^{-1} resulting in an increased yield of **4** relative to **3** for this reaction protocol.

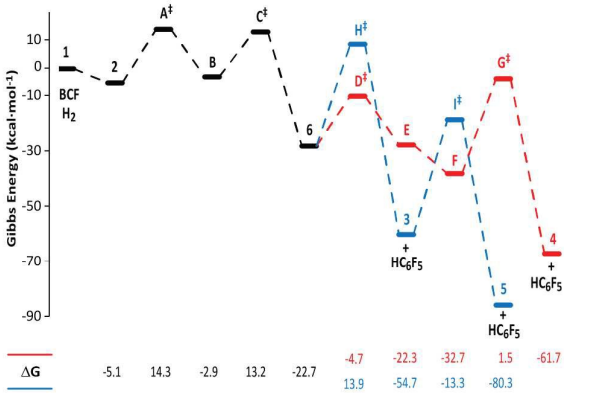

Figure 5. Reaction coordinate diagram for the conversion of **1** to products **4,5** and HC_6F_5 using $B(C_6F_5)_3/H_2$, computed at the PW6B95/def2-TZVP (COSMO-RS, toluene)//PBEh-3c level.

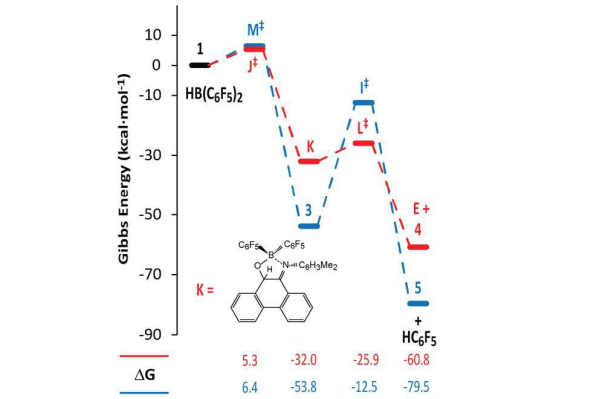

Figure 6. Reaction coordinate diagram for the conversion of **1** to products **4**, **5**, and HC_6F_5 using $HB(C_6F_5)_2$, computed at the PW6B95/def2-TZVP (COSMO-RS, toluene)//PBEh-3c level ($C_6H_3Me_2$ = 2,6-dimethylphenyl).

Efforts to extend the above reactivity to homologous α-diimines were undertaken. Reaction of (N,N'-(2,6-dimethyl)phenyl)phenanthrene-9,10-diimine **7** (**Error! eference source not found.**) with $B(C_6F_5)_3$ affords the weak adduct $C_{14}H_8(NC_6H_3Me_2)(N(C_6H_3Me_2)B(C_6F_5)_3)$ **8**, while addition of H_2 prompts reduction of the diimine to the give the α-diamine, $C_{14}H_8(NHC_6H_3Me_2)_2$ **9** quantitatively (see ESI for structural characterization). While combination of compounds **7** and **9** showed no evidence of conproportionation (see ESI), **7** did react with $HB(C_6F_5)_2$ to give a new species **10** (Scheme). ^{19}F

Dalton Transactions Accepted Manuscript

This journal is © The Royal Society of Chemistry 20xx

View Article Online
DOI: 10.1039/C7DT01024A

Published on 28 March 2017. Downloaded by University of Newcastle on 28/03/2017 21:38:16.

NMR spectra of **10** obtained at elevated temperatures (25-100 °C) showed averaging of signals, consistent with hindered rotation about the B–N bond. While purification of the crude product was achieved by sublimation (79% isolated yield), single crystals of **10** were obtained from CH_2Cl_2/pentane layered solution stored at -35°C. The resulting crystallographic study confirmed the identity of **10** as $C_{14}H_8(NHC_6H_3Me_2)(N(C_6H_3Me_2)B(C_6F_5)_2)$ (**Error! Reference ource not found.**, Figure 7a). In this α-amino borylamide, the average distance between the H(N) atom and the nearest perfluorophenyl *ipso*-carbon for the two molecules of the asymmetric unit was found to be 3.98(3) Å, considerably longer than that seen in **3**.

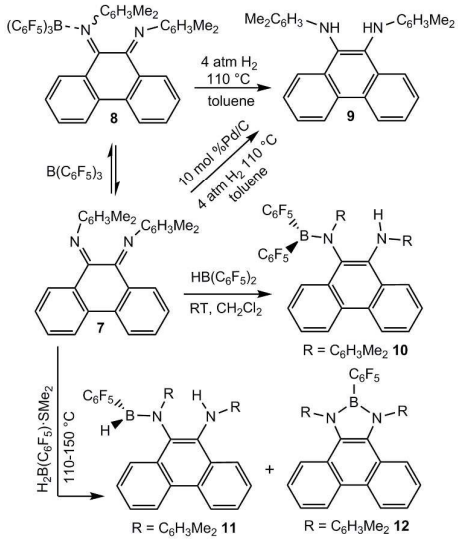

Scheme 4. Reactions of compound **7** involving $B(C_6F_5)_3/H_2$, $HB(C_6F_5)_2$, and $H_2B(C_6F_5)\cdot SMe_2$ ($C_6H_3Me_2$ = 2,6-dimethylphenyl).

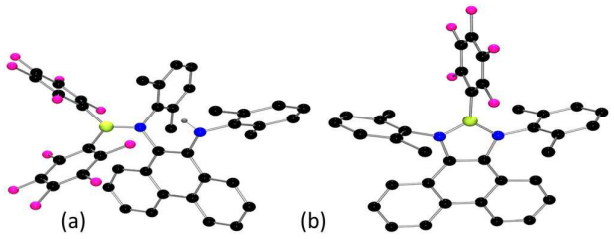

Figure 7. POV-ray depictions of (a) **11** and (b) **12**. Disordered solvent molecules (a, toluene; b, CH_2Cl_2) and C–H atoms have been omitted for clarity. Atom colour scheme: H: grey; B: yellow-green; C: black; N: blue; F: pink.

While heating of **9** with $B(C_6F_5)_3$ or pure **10** resulted in no reaction (>4 days, 150 °C), **7** reacts with $H_2B(C_6F_5)\cdot SMe_2$ (Scheme) to generate the mono-hydroborated species $C_{14}H_8(NHC_6H_3Me_2)(NC_6H_3Me_2)BH(C_6F_5)$ **11** and the 1,3,2-diazaborole $C_{14}H_8(NC_6H_3Me_2)_2BC_6F_5$ **12** (**Error! Reference ource not found.**). The two products could not be readily separated, though single crystals suitable for X-ray diffraction studies of **12** were successfully grown from a concentrated CH_2Cl_2 solution cooled to -35 °C. The molecular structure of **12** (Figure 7b) is typical of a 1,3,2-diazaborole, with B–N distance of 1.419(5) Å and N-B-N angle of 107.2(3)°. It is noteworthy that prolonged heating at 150 °C in bromobenzene did not promote conversion of the monohydroborated species **11** to compound **12**. This suggests that the geometry of the initial hydroboration product determines the elimination of H_2, consistent with the steric demands associated with rotation about the boron-substituted N-C bond.

Computations of the Gibbs energies of reactions of **7** (see ESI) reveal that access to the 2,6-dimethylphenyl-substituted 1,3,2-diazaborocyclic radical is thermodynamically feasible. However, the experimental isolation of compounds **10** and **11** suggests that steric demands result in an elevated energy for the transition state towards loss of HC_6F_5 and, thus, the corresponding diazaborocyclic radical. To probe this hypothesis, the less encumbered phenanthrene α-diimine, $C_{14}H_8(NC_6H_4Me)_2$ (**13**), bearing a *p*-tolyl substituent at nitrogen was prepared. Equimolar reactions of $B(C_6F_5)_3$ and compound **13** formed the adduct $C_{14}H_8(NC_6H_4Me)(NC_6H_4Me(B(C_6F_5)_3))$ (**14**) at ambient temperature (Scheme).

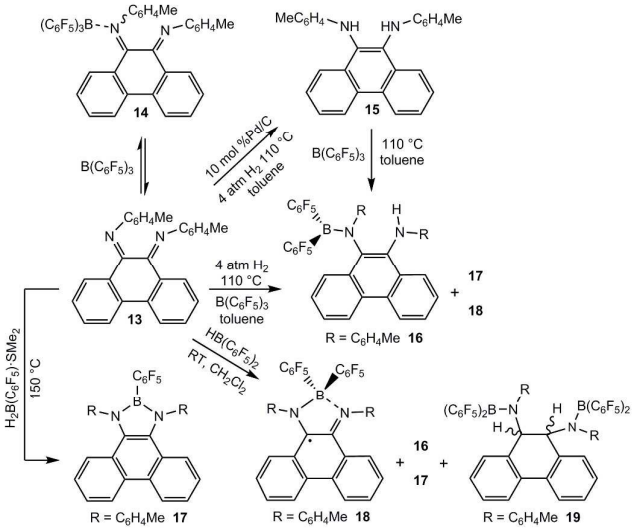

Scheme 5. Reactions of compound **13** with $B(C_6F_5)_3/H_2$, $HB(C_6F_5)_2$, and $H_2B(C_6F_5)\cdot SMe_2$ (C_6H_4Me = *p*-tolyl).

Reaction of **13** with $B(C_6F_5)_3/H_2$ heated to 110 °C for 1-2 h gave a mixture of products, including trace amount of the α –diamine, $C_{14}H_8(NHC_6H_4Me)_2$ **15**. Flash column chromatography of the crude hydrogenation reaction (95:5 pentane/CH_2Cl_2 eluent) gave partial separation, affording severals fractions containing a mixture of two species formulated as $C_{14}H_8(NHC_6H_4Me)(NC_6H_4Me(B(C_6F_5)_2)$ **16** and the 1,3,2-diazaborole, $C_{14}H_8(NC_6H_4Me)_2B(C_6F_5)$ **17**. While single crystals of **16** could not be isolated, ^{19}F and ^{11}B NMR resonances and DART-MS data support its formulation as an analog of the α-amino boryl amide **10**. The identity of **17** was confirmed by its direct synthesis from the reaction of **13** and $H_2B(C_6F_5)\cdot SMe_2$, affording **17** in 62 % isolated yield (Scheme 5) and its subsequent characterization by X-ray crystallography (

Figure **8**a). The remaining fractions from the hydrogenation reaction cumulatively yielded a trace amount of the radical $[C_{14}H_8(NC_6H_4Me)_2B(C_6F_5)_2]^{\bullet}$ **18** as evidenced by DART-MS and

Dalton Transactions Accepted Manuscript

Please do not adjust margins

View Article Online
DOI: 10.1039/C7DT01024A

Published on 28 March 2017. Downloaded by University of Newcastle on 28/03/2017 21:38:16.

EPR spectroscopy. Nonetheless, there was insufficient material for bulk isolation.

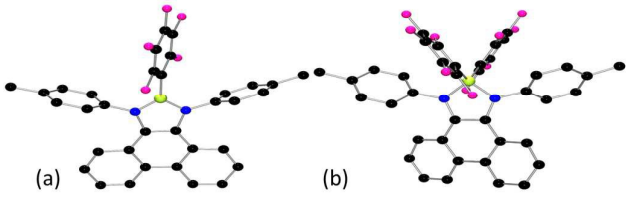

Figure 8. POV-ray depictions of (a) **17** and (b) **18**. C–H atoms have been omitted for clarity. Atom colour scheme: H: grey; B: yellow-green; C: black; N: blue; F: pink.

Efforts to generate the radical **18** by reaction of the semidiimine radical $[C_{14}H_8(NHC_6H_4Me)(NC_6H_4Me)]^{\bullet}$ derived from conproportionation of **13** and **15** afforded undentified products. However, reaction of **13** with Piers' borane (Scheme 5**Scheme**) at ambient temperature, following flash column chromatography (95:5 pentane/CH_2Cl_2 eluent), yields fractions containing **16**, **17**, **18** and a new compound **19**. Heating the crude reaction mixture to 110°C for 2-4 h prior to chromatography appears to convert **16** to **17** and HC_6F_5, while compounds **18** and **19** presist. Through mass spectrometric analysis (DART, EI) compound **19** was identified as $C_{14}H_{10}(N(C_6H_3Me_2)B(C_6F_5)_2)_2$, a minor product (<5 % isolated yield) from double hydroboration of compond **13**. While single crystals could not be obtained, compound **19** was comprehensively characterized by NMR spectroscopy (see ESI).

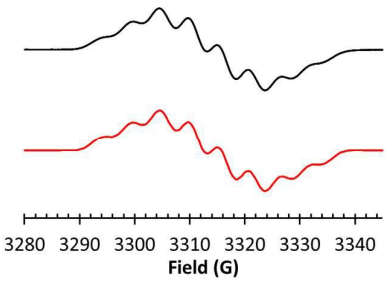

Figure **9**. Experimental X-band EPR spectrum of **18** in toluene at 298 K (black: mod. amp. = 1) and simulated EPR spectrum (red line: g = 2.0044; $a(^{11}B)$ = 5.06 G, $a(^{14}N)$ = 5.25, 4.63 G (2N), $a(^{1}H)$ = 0.83-2.12 G (8H)).

The 1,3,2-diazaborocyclic radical **18** was isolated in 14 % yield as a violet microcrystalline material. In contrast to the 1,3,2-oxazaborocyclic radical **4**, radical **18** exhibits ^{11}B and ^{19}F NMR characteristics consistent with a pseudo-tetracoordinate boron environment. Compound **18** affords magenta coloured solutions in CH_2Cl_2 that exhibit multiple absorption bands (λ =523, 562, 666nm; 1.7-6.4 x 10^3 $L{\cdot}cm^{-1}{\cdot}mol^{-1}$, see ESI) in the visible region. EPR studies (Figure 9) reveal that while hyperfine coupling constants to B and N are greater than those seen for **4** and the related dioxoborocyclic radicals,[29] the hyperfine coupling to H nuclei in **18** are smaller. This infers that the unpaired spin density is delocalized over the phenanthrene backbone to a lesser extent for **18** in comparison to **3** and the dioxo-analog. This view is supported by calculated models of the SOMO and spin density distribution (Figure 10). The measured cyclic voltammogram of compound **18** (see ESI) shows a reversible 1-electron reduction process with $E_{1/2}$ = -0.94 V (*vs*. Fc/Fc^+). The decreasing redox potentials for the dioxo-, oxaza-, and diazaborocyclic radicals indicates that incorporation of N-atoms in the borocyclic radical framework is consistent with the diminishing reduction ability of the boron radicals. The radical **18** and its solutions exhibit remarkable stability, remaining unaffected by wet and oxygenated benchtop solvents for up to 5 days and an indefinite amount of time in the solid state under an inert atmosphere of N_2.

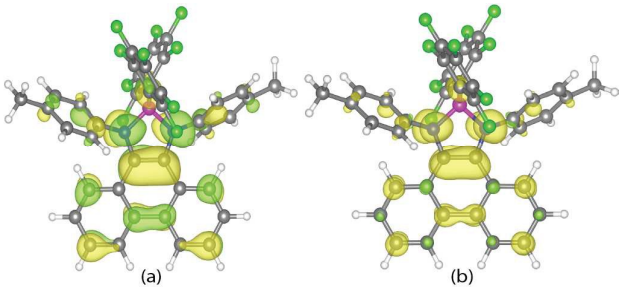

Figure 10. Calculated SOMO (a) and spin density (b) of compound **18**. Contour surface value: 0.03 a.u. and 0.002 a.u., respectively. Computational level: PW6B95/def2-TZVP//PBEh-3c. Atom colour scheme: H: white; B: pink; C: black; O: red; F: green.

Conclusions

A selection of non-innocent *o*-iminoquinone and α-diimine ligands have been shown to produce stable 1,3,2-oxaza- and diazaborocyclic radicals in FLP-type hydrogenations with $B(C_6F_5)_3$, or in hydroboration reactions with $HB(C_6F_5)_2$. The mechanism for the formation of these radicals has been comprehensively modelled through DFT-calculations and corroborated with control reactions involving independently synthesized intermediates and by-products. Whereas the *o*-iminoquinone was found to produce the targeted oxazaborocyclic radical (**4**) in either FLP-hydrogenation or hydroboration reactions, only the hydroboration route proved effective for the less sterically hindered of the two α-diimine substrates studied and yielded isolable diazaborocyclic radical **18**. The radicals afforded from these reactions represent rare examples of structurally-authenticated and comprehensively characterized polyaromatic borocyclic radicals. The key intermediate in the FLP hydrogenation pathway is postulated to be the free semiiminoquinone or semidiimine radical while the hydroboration route to borocyclic radicals is believed to involve oxidation of 1,2-hydroborated intermediates by unreacted *o*-iminoquinone or α-diimine substrates. The inability of the bulky 2,6-dimethylphenyl N-substituted α-diimine to produce a diazaborocyclic radical is attributed to a steric limitation. Efforts to extend these synthetic approaches to radicals containing other group 13 elements as well as to explore the properties and reactivity of such borocyclic radicals are on-going and will be reported in due course.

Dalton Transactions Accepted Manuscript

This journal is © The Royal Society of Chemistry 20xx

Please do not adjust margins
View Article Online
DOI: 10.1039/C7DT01024A

Published on 28 March 2017. Downloaded by University of Newcastle on 28/03/2017 21:38:16.

Experimental Section

Materials and general methods All preparative procedures were performed in an inert atmosphere of dry, deoxygenated (O_2 < 0.5 ppm) nitrogen, using glovebox techniques or standard Schlenk techniques unless otherwise specified. Solvents were stored over activated 4 Å molecular sieves following drying procedures. Pentane, dichloromethane, and toluene (Sigma Aldrich) were dried using a Grubbs-type Innovative Technologies solvent purification system. Bromobenzene was dried over and distilled from CaH_2. Deuterated solvents ($CDCl_3$, toluene-d8) were purchased from Cambridge Isotope Laboratories, Inc. and stored over activated 4 Å molecular sieves. 9,10-phenanthrenequinone (>95% purity), *p*-toluidine, titatnium (IV) chloride (puriss) and activated Pd/C were obtained from Sigma Aldrich and used without further purification. 9,10-phenanthrenequinone (>90% purity) was obtained from Alfa Aesar. $B(C_6F_5)_3$ was purchased from Boulder Scientific and sublimed under vacuum at 95 °C prior to use. 2,6-dimethylaniline was obtained from Acros Organics. *N*-(2,6-dimethylphenyl)-phenanthren-*o*-iminoquinone (**1**), *N*,*N*'-(2,6-dimethylphenyl)-phenanthrene-9,10-diimine (**7**), *N*,*N*'-(*p*-tolyl)-phenanthrene-9,10-diimine (**13**), $HB(C_6F_5)_2$, and $H_2B(C_6F_5)\cdot SMe_2$ were prepared according to previously reported synthetic procedures.[51,52,53,37] *o*-Iminoquinone and α-diimine substrates were purified by column chromatography using Silicycle Silia-P Flash Silica Gel. A Nanochem Weldassure purifier column was used to dry H_2 (grade 5.0, supplied by Linde) used in hydrogenation reactions. Thin-layer chromatography (TLC) was performed on EMD Silica Gel 60 F_{254} aluminum plates and visualization of the developed plates was achieved using a UV lamp (254 nm). Silica gel used in glovebox manipulations was dried under vacuum at 150 °C and plastic syringes were used in place of glass columns.

All NMR spectra were collected at 298 K on Bruker Avance III 400, Agilent DD2 500, or Agilent DD2 600 spectrometers in 3 or 5 mm diameter NMR tubes. ^{1}H and ^{13}C NMR chemical shifts are reported relative to protio-solvent signals, while ^{11}B and ^{19}F NMR chemical shifts are reported relative to $(Et_2O)BF_3$ and $CFCl_3$ external standards, respectively. For compounds generated *in situ* only ^{11}B and ^{19}F NMR data are reported, while isolated compounds are accompanied by additional ^{1}H and $^{13}C\{^1H\}$ NMR data. All chemical shifts (δ) are reported in ppm and coupling constants are given in Hz (see ESI for atom numbering). Departmental facilities were used for all elemental analyses (Perkin Elmer 2400 Series II CHNS Analyser) and high resolution mass spectrometry (HRMS-DART; JEOL AccuTOF).

Generation of $C_{14}H_8O(NC_6H_3Me_2)B(C_6F_5)_3$ (2). *Attempts to isolate this species were unsuccessful.* A green-brown solution in toluene, prepared by combining equimolar amounts of compound **1** and $B(C_6F_5)_3$ at ambient temperature in an NMR tube. ^{11}B NMR (128 MHz, toluene-d8, 298 K): δ 39.5 (br s); ^{19}F NMR (377 MHz, toluene-d8, 298 K): δ -130.5 (br s, 6F, *o*-C_6F_5), -147.6 (br s, 3F, *p*-C_6F_5), -161.5 (br s, 6F, *m*-C_6F_5).

Generation of $C_{14}H_8O(NHC_6H_3Me_2)B(C_6F_5)_2$ (3). *Method 1*: $B(C_6F_5)_3$ (154 mg, 0.3 mmol) was dissolved in a minimum of toluene (2 mL) and transferred to a 50 mL Schlenk bomb containing a stir bar. The vial containing remnant $B(C_6F_5)_3$ was rinsed with fresh toluene (3 x 1 mL) and these aliquots were transferred to a vial of **1** (93 mg, 0.3 mmol) and the combined solution subsequently transferred to the Schlenk bomb. The solution, containing the adduct of **1** and $B(C_6F_5)_3$, appeared dark green-brown. The bomb was degassed using three freeze-pump-thaw cycles prior to the addition of H_2 (4 atm) at -196 °C. The solution was subsequently heated to 110 °C for 1 h, resulting in a dark brown homogenous solution, which was cooled to room temperature and dried *in vacuo*. The solid obtained was dark brown. *Method 2*: A solution of compound **1** (93 mg, 0.3 mmol) in DCM (2 x 0.5 mL) was added to a concentrated solution of $HB(C_6F_5)_2$ (104 mg, 0.3 mmol) in DCM (1 mL) while stirring. Instantaneously the mixture exhibited a dark brown colour. The homogenous solution was stirred for 1 h prior to removal of volatiles under reduced pressure, furnishing a dark brown solid. *Method 3*: A solution of compound **6** (94 mg, 0.3 mmol) in DCM (2 x 0.5 mL) was added to a solution of $B(C_6F_5)_3$ (153 mg, 0.3 mmol) in DCM (1 mL), with stirring. The mixture immediately produced a light brown coloured solution. The solution was left to stir for 0.5 h prior to removal of volatiles under reduced pressure, furnishing a brown solid. Compound **3** eliminates HC_6F_5 over time, in solution, to give compound **5**. Attempts to crystallize compound **3** from large scale syntheses by any of the three above methods consistently resulted in mixtures of compounds **3** and **5**. Crystals of **3** suitable for X-Ray diffraction were obtained by slow evaporation of a dilute pentane solution over a span of 3 days at ambient temperature inside an inert atmosphere glovebox. The solution was decanted, affording bronze crystals (~15 mg). ^{11}B NMR (128 MHz, $CDCl_3$, 298 K): δ 10.0 (br s); ^{19}F NMR (377 MHz, $CDCl_3$, 298 K): δ -131.9 (br s, 1F, *o*-C_6F_5), -137.0 (br s, 1F, *o*-C_6F_5), -155.8 (br pseudo d, 2F, *p*-C_6F_5), -162.6 (br s, 2F, *m*-C_6F_5), -164.0 (br s, 2F, *m*-C_6F_5); HRMS (DART) calcd for $[C_{34}H_{19}BF_{10}NO]$ ($[M+H]^+$) 658.1400, Found 658.1406.

Synthesis of $[C_{14}H_8O(NC_6H_3Me_2)B(C_6F_5)_2]^\bullet$ (4). *Method 1*: Following the same procedure as for compound **3** (*method 1*), and using the same quantities of reagent, the reaction mixture was heated to 110 °C for 3 h, resulting in a dark brown homogenous solution. The solution was cooled to room temperature and dried *in vacuo*. The solid obtained was dark brown. Crystalline material, grown from concentrated DCM solutions cooled to -35 °C, was decanted, washed with cold pentane and successively recrystallized in this fashion until spectroscopically pure and X-ray diffraction quality dark brown crystals of compound **4** were obtained. Isolated yield: 26 mg, 13 % (crystals). *Method 2*: Following a similar procedure as used for compound **3** (*method 2*), and using the same quantities of reagent, compound **1** and $HB(C_6F_5)_2$ were combined in 3 mL toluene. The mixing immediately gave the solution a dark brown colouration. The homogenous reaction mixture was heated to 110 °C and left to stir for 3 h prior to removal of volatiles under reduced pressure at room temperature, furnishing a dark brown solid. Following fractional crystallization, dark brown microcrystals were

Dalton Transactions Accepted Manuscript

Please do not adjust margins

View Article Online
DOI: 10.1039/C7DT01024A

Published on 28 March 2017. Downloaded by University of Newcastle on 28/03/2017 21:38:16.

obtained. Isolated yield: 37 mg, 18 % (crystals). ^{1}H NMR (400 MHz, $CDCl_3$, 298 K): NMR silent; ^{19}F NMR (377 MHz, $CDCl_3$, 298 K): δ -159.9 (br s, C_6F_5); ^{11}B NMR (128 MHz, $CDCl_3$, 298 K): NMR silent; $^{13}C\{^1H\}$ NMR (101 MHz, $CDCl_3$, 298 K): NMR silent; HRMS (DART) calcd for $[C_{34}H_{17}BF_{10}NO]$ ($[M]^+$) 656.1243, found 656. 1257; Elemental Analysis calcd (%) $C_{34}H_{17}BF_{10}NO{\cdot}1/2(CH_3CH_2CH_2CH_2CH_3)$: C 63.32; H 3.35; N 2.02; Found: C 63.58; H 3.43; N 2.45.

Synthesis of $C_{14}H_8O(NC_6H_3Me_2)BC_6F_5$ (5). $H_2B(C_6F_5){\cdot}SMe_2$ (73 mg, 0.3 mmol) was dissolved in a minimum of DCM (1 mL) and added to a vial of compound **1** (93 mg, 0.3 mmol) in 0.5 mL DCM, equipped with a stir bar. A further 0.5 mL of DCM was used to quantitatively transfer the remaining $H_2B(C_6F_5){\cdot}SMe_2$ to the reaction mixture. Within several minutes of initial mixing the reaction exhibited a teal-green colour. Over the course of 1 h stirring at ambient temperature the reaction turned colourless, and then became a faintly yellow, clear solution. The reaction mixture was subsequently concentrated *in vacuo* and stored at -35 °C, affording colourless crystals suitable for X-Ray diffraction; yield: 131 mg, 89 % (crystal). Crude material (faintly yellow in colour) from larger scale syntheses may alternatively be purified by sublimation under reduced pressure with heating (~163 °C). ^{1}H NMR (500 MHz, $CDCl_3$, 298 K): δ 8.79 (d, $^{3}J_{HH}$ = 8.6 Hz, 1H, H_9), 8.75 (d, $^{3}J_{HH}$ = 8.2 Hz, 1H, H_3), 8.44 (d, $^{3}J_{HH}$ = 8.1 Hz, 1H, H_6), 7.75 (tm, $^{3}J_{HH}$ = 7.6 Hz, 1H, H_5), 7.65 (tm, $^{3}J_{HH}$ = 7.6 Hz, 1H, H_4), 7.54 (tm, $^{3}J_{HH}$ = 7.6 Hz, 1H, H_{10}), 7.33 – 7.20 (m, 4H, H_{11} & H_{18} & H_{19}), 7.06 (d, $^{3}J_{HH}$ = 8.3 Hz, 1H, H_{12}), 2.12 (s, 6H, H_{17}); ^{11}B NMR (128 MHz, $CDCl_3$, 298 K): δ 28.9 (br s); $^{13}C\{^1H\}$ NMR (126 MHz, $CDCl_3$, 298 K): δ 148.0 (dm, $^{1}J_{CF}$ ~ 247 MHz, *o*-C_6F_5), 142.6 (dm, $^{1}J_{CF}$ ~ 249 MHz, *p*-C_6F_5), 142.5 (s, C_1), 137.3 (dm, $^{1}J_{CF}$ ~ 249 MHz, *m*-C_6F_5), 137.0 (s, C_{15}), 136.3 (s, C_{16}), 128.7 (s, C_{18}), 128.2 (s, C_{19}), 128.0 (s, C_8), 127.3 (two overlapping s, C_2 & C_5), 126.9 (s, C_{11}), 126.3 (s, C_{14}), 125.2 (s, C_4), 124.8 (s, C_{10}), 124.1 (s, C_{13}), 123.7 (s, C_9), 123.4 (s, C_7), 123.1 (s, C_3), 120.3 (s, C_6), 119.8 (s, C_{12}), 103.4 (br s, *i*-C_6F_5), 18.2 (s, C_{17}); ^{19}F NMR (377 MHz, $CDCl_3$, 298 K): δ -129.3(m, 2F, *o*-C_6F_5), -150.2 (tt, $^{3}J_{FF}$ = 20.2 Hz, $^{4}J_{FF}$ = 3.0 Hz, 1F, *p*-C_6F_5), -160.9 – -161.1 (m, 2F, *m*-C_6F_5); HRMS (DART) calcd for $[C_{28}H_{18}BF_5NO]$ ($[M+H]^+$) 490.1402, Found 490.1391; Elemental Analysis calcd (%)$C_{28}H_{17}BF_5NO$: C 68.74, H 3.50, N 2.86; Found: C 68.60,H 3.66, N 2.81.

Synthesis of $C_{14}H_8OH(NHC_6H_3Me_2)$ (6). Following the methods used to prepare 9,10-phenanthrene diol,[42] a 25 mL bomb containing a 3 mL toluene solution of compound **1** (93 mg, 0.3 mmol) and 10 mol% (3 mg) Pd/C was sealed and degassed using three freeze-pump-thaw cycles. The bomb was then charged with 4 atm H_2 at -196 °C and warmed to room temperature using a water bath. The solution was subsequently heated for 2 h at 110 °C and filtered through celite in the glovebox after cooling. Removal of volatiles *in vacuo* and repeated washes with cold pentane (3 x 0.5 mL) afforded an analytically pure white powder. Isolated yield: 90 mg, 96 %. X-ray diffraction quality colourless single crystals were grown from a DCM solution layered with pentane and stored at -35 °C. ^{1}H NMR (500 MHz, $CDCl_3$, 298 K): δ 8.71-8.62 (m, 2H, H_3 & H_9), 8.38 (d, $^{3}J_{H\text{-}H}$ = 7.3 Hz, 1H, H_6), 7.73-7.65 (m, 2H, H_4 & H_5), 7.61 (d, $^{3}J_{H\text{-}H}$ = 7.6 Hz, 1H, H_{12}), 7.51-7.40 (m, 2H, H_{10} & H_{11}), 7.02 (d, $^{3}J_{H\text{-}H}$ = 7.6 Hz, 2H, H_{18}), 6.86 (t, $^{3}J_{H\text{-}H}$ = 7.3 Hz, 1H, H_{19}), 5.16 (br s, OH), 2.12 (s, 3H, H_{17}); $^{13}C\{^1H\}$ NMR (126 MHz, $CDCl_3$, 298 K): δ 146.7 (s, C_1), 142.8 (s, C_{15}), 131.5 (s, C_{13}), 130.0 (s, C_7) 129.9 (s, C_{18}), 127.2 (s, C_{11}), 126.9 (s, C_4), 126.6 (s, C_5), 126.4 (s, C_8), 125.9 (s, C_{16}), 124.8 (s, C_{14}), 124.0 (s, C_{10}) 123.0 (br s, C_9 & C_6), 122.5 (s, C_3), 121.8 (s, C_{12}), 121.1 (s, C_{19}), 117.7 (s, C_2), 18.8 (s, C_{17}); HRMS (DART) calcd for $[C_{22}H_{19}NO]^+$ ($[M+H]^+$) 314.1544, found 314.1541; Elemental Analysis calcd (%) for $C_{22}H_{19}NO$: C 84.31; H 6.11; N 4.47; Found*: C 83.00; H 6.15; N4.39. Elemental analysis was consistently low for carbon.

Generation of $C_{14}H_8(NC_6H_3Me_2)(N(C_6H_3Me_2)B(C_6F_5)_3)$ (8). An orange-red solution in toluene was prepared from equimolar amounts of compound **7** and $B(C_6F_5)_3$ at room temperature. ^{11}B NMR (128 MHz, , toluene-d8, 298 K): δ 58.5 (br s); ^{19}F NMR (377 MHz, , toluene-d8, 298 K): δ -128.7 (br s, 6F, *o*-C_6F_5), -142.0 (br s, 3F, *p*-C_6F_5), -160.1 (br s, 6F, *m*-C_6F_5).

Synthesis of $C_{14}H_8(NHC_6H_3Me_2)_2$ (9). Identical to the preparation of compound **6** (125 mg, 0.3 mmol scale of compound **7**; 3 mg, 10 mol % Pd/C), only, using twice the volume of toluene (6 mL) given the reduced solubility of compound **7** in comparison with compound **1**. The crude material obtained following removal of volatiles was washed with cold pentane (3 x 0.2 mL) to give a white powder; Yield: 119 mg, 95 % (powder). Colourless single crystals of the product, used in X-Ray diffraction studies, were isolated from a DCM solution layered with pentane and stored at -35 °C. ^{1}H NMR (400 MHz, $CDCl_3$, 298 K): δ 8.65 (d, $^{3}J_{H\text{-}H}$ = 7.9 Hz, 2H, H_3/H_{12}), 7.84 (d, 2H, $^{3}J_{H\text{-}H}$ = 7.8 Hz, H_6/H_9), 7.50 (t, $^{3}J_{H\text{-}H}$ = 7.6 Hz, 2H, H_4/H_{11}), 7.41 (t, $^{3}J_{H\text{-}H}$ = 7.6 Hz, 2H, H_5/H_{10}), 6.93 (d, $^{3}J_{H\text{-}H}$ = 7.0 Hz, 4H, H_{18}), 6.82 (t, $^{3}J_{H\text{-}H}$ = 7.4 Hz, 2H, H_{19}), 5.27 (br s, N-H), 1.85 (s, 12H, H_{17}); $^{13}C\{^1H\}$ NMR (126 MHz, $CDCl_3$,298 K): δ 142.3 (s, C_{15}), 130.1 (s, C_7/C_8), 129.3 (s, C_{18}), 129.0 (s, C_2/C_{13}), 128.5 (s, C_1/C_{14}), 128.0 (s, C_{16}), 126.7 (s, C_5), 125.1 (s, C_4), 123.0 (two overlapping s, C_3/C_{12} & C_6/C_9), 121.3 (s, C_{19}), 18.9 (s, C_{17}); HRMS (DART) calcd for $[C_{30}H_{29}N_2]^+$ ($[M+H]^+$) 417.2331, found 417.2339; Elemental Analysis calcd (%) for $C_{30}H_{28}N_2$: C 86.50; H 6.78; N 6.72; Found: C 85.65; H 6.81; N 6.66. Elemental analysis was consistently low for carbon.

Synthesis of $C_{14}H_8(NHC_6H_3Me_2)(N(C_6H_3Me_2)B(C_6F_5)_2)$ (10). To separate vials containing $HB(C_6F_5)_2$ (104 mg, 0.3 mmol) and compound **7** (124 mg, 0.3 mmol) 1 mL volumes of toluene were added. Dropwise addition of the clear, colourless solution of $HB(C_6F_5)_2$ to the stirring red-orange suspension of **7** resulted in the immediate formation of a tan-orange coloured solution. The reaction mixture was left to stir for 4 h before removal of volatiles *in vacuo*. The crude product was purified by flash column chromatography (eluent = 7:3 pentane:DCM). Yield: 180.2 mg, 79 % (yellow powder). A concentrated DCM solution of the product layered with pentane and stored at -35 °C readily yielded pale yellow crystals suitable for X-ray diffraction. ^{1}H NMR (500 MHz, $CDCl_3$, 298 K): δ 8.60 (dm, $^{3}J_{HH}$ = 8.4 Hz, 1H, H_9), 8.56 (dm, $^{3}J_{HH}$ = 8.5 Hz, 1H, H_6), 8.36 (d, $^{3}J_{HH}$ = 8.5 Hz, 1H, H_3), 7.59 (t, $^{3}J_{HH}$ = 7.3 Hz, 1H, H_4), 7.55–7.49 (overlapping tm & d, 2H, H_{10} & H_{12}), 7.45 (tm, $^{3}J_{HH}$ = 7.5 Hz, 1H, H_5), 7.19 (tm, , $^{3}J_{HH}$ = 7.6 Hz,1H, H_{11}), 7.10 (d, $^{3}J_{HH}$ = 7.6 Hz, 1H, $H_{18b/a}$), 6.89–6.72 (m, 4H, H_{18c} & H_{18d} & H_{19a} & H_{19c}), 6.64 (d,

Dalton Transactions Accepted Manuscript

This journal is © The Royal Society of Chemistry 20xx

Please do not adjust margins
View Article Online
DOI: 10.1039/C7DT01024A

Published on 28 March 2017. Downloaded by University of Newcastle on 28/03/2017 21:38:16.

$^3J_{HH}$ = 7.2 Hz, 1H, $H_{18a/b}$), 5.83 (br s, N-H), 2.46 (s, 3H, $H_{17a/b}$), 2.42 (s, 3H, $H_{17d/c}$), 1.89 (s, 3H, $H_{17c/d}$), 0.90 (s, 3H, $H_{17b/a}$); ^{11}B NMR (128 MHz, $CDCl_3$, 298 K): δ 40.0 (br s); $^{13}C\{^1H\}$ NMR (126 MHz, $CDCl_3$, 298 K, $CDCl_3$): δ 147.8 (dm, $^1J_{CF}$ ~ 258 MHz, *o*-C_6F_5), 147.4 (dm, $^1J_{CF}$ ~ 246 MHz, *o*-C_6F_5), 146.3 (dm, $^1J_{CF}$ ~ 248 MHz, *o*-C_6F_5), 145.8 (dm, $^1J_{CF}$ ~ 255 MHz, *o*-C_6F_5), 142.2 (dm, $^1J_{CF}$ ~ 256 MHz, *p*-C_6F_5), 141.6 (dm, $^1J_{CF}$ ~ 256 MHz, *p*-C_6F_5), 141.6 (s, C_{15c}), 140.5 (s, C_{15a}), 136.9 (br dm, $^1J_{CF}$ ~ 245 MHz, *m*-C_6F_5), 135.6 (s, $C_{16a/b}$), 135.42 (s, $C_{16c/d}$), 134.1 (s, $C_{16b/a}$), 130.6 (s, $C_{18c/d}$), 130.5 (s, C_2), 129.9 (s, C_8), 129.7 (s, C_{13} or C_{14}), 129.4 (s, $C_{18a/b}$), 129.1 (s, s, C_{14} or C_{11}), 128.8 (s, C_{19c}), 128.6 (s, $16_{d/c}$), 128.6 (s, $C_{18b/a}$), 127.0 (s, C_{10}), 126.9 (s, C_7), 126.6 (s, $18_{d/c}$), 126.3 (s, C_{11}), 126.0 (s, C_4), 125.8 (s, C_1), 124.3 (s, C_5), 124.3 (br t, C_3), 123.8 (s, C_{12}), 122.9 (s, C_6), 122.7 (s, C_9), 122.5 (s, C_{19a}), 112.9 (br s, *i*-C_6F_5), 21.8 (d, J_{CF} ~ 6 Hz, $C_{17c/d}$), 20.0 (br t, $C_{17d/c}$), 19.1 (d, J_{CF} ~ 3 Hz, $C_{17b/a}$), 17.4 (s, $C_{17a/b}$); ^{19}F NMR (377 MHz, $CDCl_3$, 298 K): δ -128.0 (dm, $^3J_{FF}$ = 24 Hz, 1F, *o*-C_6F_5(a/b)), -130.9 (dm, $^3J_{FF}$ = 24Hz, 1F, *o*-C_6F_5(c/d)), -131.7 (dm, $^3J_{FF}$ = 24 Hz, 1F, *o*-C_6F_5(b/a)), -132.8 (dm, $^3J_{FF}$ = 24Hz, 1F, *o*-C_6F_5(d/c)), -150.3 (t, $^3J_{FF}$ = 20 Hz, 1F, *p*-C_6F_5(a)), -151.1 (t, $^3J_{FF}$ = 20 Hz, 1F, *p*-C_6F_5(c)), -160.8 – -161.4 (m, 4F, *m*-C_6F_5(a,b,c,d)); HRMS (DART) calcd for $[C_{42}H_{28}BF_{10}N_2]$ ($[M+H]^+$) 761.2186, Found 761.2186; Elemental Analysis calcd (%) $C_{42}H_{27}BF_{10}N_2$: C 66.33, H 3.58, N 3.68; Found: C 64.93,H 3.59, N 3.57. Elemental analysis was consistently low for carbon.

Generation of $C_{14}H_8(NC_6H_3Me_2)_2BC_6F_5$ (12). Similar to the preparation of compound **5** (128 mg, 0.31 mmol of compound **7**; 76 mg, 0.31 mmol of $H_2B(C_6F_5)\cdot SMe_2$), but owing to the reduced solubility of compound **7** in comparison with compound **1**, a greater volume of toluene (3 mL) was used. After heating for 1 h at 110 °C, compounds **11** and **12** were formed. Solutions containing mixtures of **11** and **12** were yellow in colour. Single crystals used in X-ray crystallography studies were obtained from a concentrated DCM solution stored at -35 °C. Attempted separation of compounds **11** and **12** by sublimation, fractional crystallization, flash column chromatography, and repeated washing failed, precluding their complete characterization. ^{11}B NMR (128 MHz, $CDCl_3$, 298 K): δ 25.3 (br s); ^{19}F NMR (377 MHz, $CDCl_3$, 298 K): δ -128.3 (dd, $^3J_{FF}$ = 23 Hz, $^4J_{FF}$ = 9 Hz, 2F, *o*-C_6F_5), -151.7 (t, $^3J_{FF}$ = 21 Hz, 1F, *p*-C_6F_5), -161.6 (td, $^3J_{FF}$ = 23 Hz, $^4J_{FF}$ = 9 Hz, 2F, *m*-C_6F_5) ; HRMS (DART) calcd for $[C_{36}H_{27}BF_5N_2]$ ($[M+H]^+$) 593.2187, Found 593.2199.

Generation of $C_{14}H_8(NC_6H_4Me)(NC_6H_4Me(B(C_6F_5)_3))$ (14). A dark green solution in toluene, prepared from equimolar amounts of compound **13** and $B(C_6F_5)_3$. ^{11}B NMR (128 MHz, toluene-d8, 298 K): δ 2.6 (br s), 11.9 (s); ^{19}F NMR (377 MHz, toluene-d8, 298 K): δ -131.8 – -134.1 (br m, 6F, *o*-C_6F_5), -158.5 (br s, 3F, *p*-C_6F_5), -164.6 (br s, 6F, *m*-C_6F_5).

Synthesis of $C_{14}H_8(NHC_6H_4Me)_2$ (15). Identical to the preparation of compounds **6** and **9** (121 mg, 0.3 mmol of compound compound **13**; 3 mg, 10 mol% Pd/C) using 4 mL of toluene and heating the reaction mixture to 110 °C for 1 h. The crude material obtained from filtration over Celite and removal of volatiles *in vacuo* was washed with cold pentane (3 x 0.2 mL) to give a bright yellow powder; Yield: 89.4 mg, 92 % (powder). Yellow single crystals of the product, used in X-Ray diffraction studies, were isolated from a DCM solution layered with pentane and stored at -35 °C. The product is stable under the inert atmosphere of the glovebox for an indefinite amount of time, however, trace amounts of O_2 causes clear, yellow solutions of **15** to oxidize and turn dark purple over the course of 5-6 h (see ESI for further description of stability). ^{1}H NMR (500 MHz, $CDCl_3$, 298 K): δ 8.74 (d, $^3J_{HH}$ = 8.4 Hz, 2H, H_3/H_{12}), 8.03 (d, $^3J_{HH}$ = 8.1 Hz, 2H, H_6/H_9), 7.63 (t, $^3J_{HH}$ = 7.9 Hz, 2H, H_4/H_{11}), 7.53 (t, $^3J_{HH}$ = 7.6 Hz, 2H, H_5/H_{10}), 6.96 (d, $^3J_{HH}$ = 8.2 Hz, 4H, H_{17}), 6.57 (d, $^3J_{HH}$ = 8.0 Hz, 4H, H_{16}); 2.26 (s, 6H, H_{19}), $^{13}C\{^1H\}$ NMR (126 MHz, $CDCl_3$, 298 K): δ 144.4 (s, C_{15}), 130.2 (s, C_1/C_{14}), 130.0 (s, C_7/C_8), 129.9 (br m, C_{17} & C_2/C_{13}), 128.9 (s, C_{18}), 126.9 (s, $C_{5/10}$), 126.3 (s, C_4/C_{11}), 125.1 (br s, C_6/C_9), 123.0 (s, C_3/C_{12}), 115.6 (s, C_{16}), 20.6 (s, C_{19}); (DART) calcd for $[C_{28}H_{25}N_2]$ ($[M+H]^+$) 389.2018 , Found 389.2013; Elemental Analysis calcd (%) $C_{28}H_{24}N_2.C_7H_8$: C 87.46, H 6.71, N 5.83; Found: C 85.14, H 6.45, N 6.34. Elemental analysis was consistently low for carbon and solid samples handled (~ 5 minutes) under an inert atmosphere of N_2 for elemental analysis repeatedly reverted to compound **12** due to trace oxygen.

Generation of $C_{14}H_8(NHC_6H_4Me)(NC_6H_4Me(B(C_6F_5)_2)$ (16). Similar to the preparation of compound **3** (*method 1*) (156 mg, 0.31 mmol of $B(C_6F_5)_3$; 126 mg, 0.33 mmol compound **13**), but owing to the reduced solubility of compound **13** in comparison with compound **1**, a greater volume of toluene (5 mL) was used. The flask charged with hydrogen gas was subsequently heated to 110 °C for 2 h, resulting in a dark red homogenous solution, which was cooled to room temperature and dried *in vacuo*. The solid obtained was dark magenta. Complete separation from compound **18** was achieved by flash column chromatography (eluent = 95:5 pentane:DCM). Compounds **16** and **17** could not be separated by column chromatography, fractional crystallisation, or sublimation (see ESI). ^{11}B NMR (128 MHz, $CDCl_3$, 298 K): δ 36.0 (br s); ^{19}F NMR (377 MHz, $CDCl_3$, 298 K): δ -129.1 (m, 1F, *o*-C_6F_5), -131.4 (br d, $^3J_{FF}$ = 24.7 Hz, 1F, *o*-C_6F_5), -132.7 (br d, $^3J_{FF}$ = 21.6 Hz, 1F, *o*-C_6F_5), -133.3 (m, 1F, *o*-C_6F_5), -151.4 (t, $^3J_{FF}$ = 19.8 Hz, 1F, *p*-C_6F_5), -152.0 (t, $^3J_{FF}$ = 20.4 Hz ,1F, *p*-C_6F_5), -159.9 (m, 1F, *m*-C_6F_5), -160.7 (m, 1F, *m*-C_6F_5), -161.4 (ddd, $^3J_{FF}$ = 24.7 Hz & 20.0 Hz, $^4J_{FF}$ = 10.2 Hz, 1F, *m*-C_6F_5), -161.8 (ddd, $^3J_{FF}$ = 24.2 Hz & 19.8 Hz, $^4J_{FF}$ = 9.7 Hz, 1F, *m*-C_6F_5). HRMS (DART) calcd for $[C_{40}H_{24}BF_{10}N_2]$ ($[M+H]^+$) 733.1873, Found 733.1872.

Synthesis of $C_{14}H_8(NC_6H_4Me)_2B(C_6F_5)$ (17). Identical to the preparation of compound **12** (123 mg, 0.32 mmol of compound **13**; 79 mg, 0.33 mmol of $H_2B(C_6F_5)\cdot SMe_2$) using 4 mL of bromobenzene and heating the reaction mixture to 150 °C for 3 h. immediately forming a dark red-orange coloured solution. The solution changes from a dark red-orange colour solution (room temperature) to pale yellow with heating. Unreacted compound **13** could not be removed by washing or recrystallization, however filtration of the crude reaction mixture through silica gel using a 95:5 pentane:DCM eluent furnished pure compound **17** in 62 % (yellow powder). Single crystals suitable for X-ray crystallography were grown at -35 °C from a concentrated DCM solution. ^{1}H NMR (600 MHz, $CDCl_3$, 298 K): δ 8.75 (br d, $^3J_{HH}$ = 8.8 Hz, 2H, H_3/H_{12}), 7.45 (ddd, $^3J_{HH}$ =

Dalton Transactions Accepted Manuscript

Please do not adjust margins

View Article Online
DOI: 10.1039/C7DT01024A

Published on 28 March 2017. Downloaded by University of Newcastle on 28/03/2017 21:38:16.

8.3 Hz, $^3J_{HH}$ = 6.9 Hz, $^4J_{HH}$ = 1.3 Hz, 2H, H_4/H_{11}), 7.34 (dd, $^3J_{HH}$ = 8.5 Hz, $^4J_{HH}$ = 1.2 Hz, 2H, H_6/H_9), 7.18-7.29 (m, 10H, H_5 & H_{16} & H_{17}), 2.43 (s, 6H, H_{19}); ^{11}B NMR (128 MHz, $CDCl_3$, 298 K): δ 25.9 (br s); $^{13}C\{^1H\}$ NMR (126 MHz, $CDCl_3$, 298 K): δ 139.3 (s, C_{15}), 137.2 (s, C_{18}), 130.2 (s, C_{17}), 127.9 (s, C_7/C_8), 127.9 (s, C_2/C_{13}), 127.4 (s, C_{16}), 126.0 (s, C_8/C_{10}), 124.1 (s, C_1/C_{14}), 123.9 (s, C_4/C_{11}), 123.7 (s, C_3/C_{12}), 122.1 (s, C_6/C_9), 21.4 (s, C_{19}); ^{19}F NMR (377 MHz, $CDCl_3$, 298 K): δ -129.1 (dd, , $^3J_{FF}$ = 24.5 Hz, $^4J_{FF}$ = 9.7, 2F, *o*-C_6F_5), -152.0 (t, $^3J_{FF}$ = 20.2 Hz, 1F, *p*-C_6F_5), -161.8 (ddd, , $^3J_{FF}$ = 23.9 & 19.4 Hz, $^4J_{FF}$ = 9.8 Hz, 2F, *m*-C_6F_5); HRMS (DART) calcd for $[C_{34}H_{23}BF_5N_2]$ ($[M+H]^+$) 565.1874, Found 565.1867; Elemental Analysis calcd (%) $C_{34}H_{22}BF_5N_2$: C 72.36, H 3.93, N 4.96; Found: C 72.36, H 3.93, N 4.96.

Synthesis of $[C_{14}H_8(NC_6H_4Me)_2B(C_6F_5)_2]^\bullet$ (18). Identical to the preparation of compound **4** (*method 2*) (120 mg, 0.3 mmol of compound **13**; 107 mg, 0.3 mmol of $HB(C_6F_5)_2$) using 2.5 mL toluene. The ruby red-coloured reaction mixture was left to stir at for 2 h before removal of volatiles *in vacuo*. The crude product (**18**) was a magenta colour solid and was purified by flash column chromatography (eluent = 95:5 pentane:DCM). Washing the crude product (or mixed fractions containing **16** and **17**) with cold pentane was also performed during purification. Isolated yield: 31.4 mg, 14 % (violet powder). Crystals used in X-ray diffraction studies were collected from a concentrated solution of **18** in approximately 70:30 pentane:DCM solvent mixture stored at -35 °C. ^{1}H NMR (500 MHz, $CDCl_3$, 298 K): δ NMR silent; ^{11}B NMR (128 MHz, $CDCl_3$, 298 K): δ -11.2 (br s); $^{13}C\{^1H\}$ NMR (126 MHz, 298 K): δ NMR silent ; ^{19}F NMR (377 MHz, $CDCl_3$, 298 K): δ -136. 8 (br s, 4F, *o*-C_6F_5), -158.8 (t, $^3J_{F\text{-}F}$ = 18.1 Hz, 2F, *p*-C_6F_5), -161.8 (tm, $^3J_{F\text{-}F}$ = 22.0 Hz, 4F, *m*-C_6F_5); HRMS (DART) calcd for $[C_{40}H_{23}BF_{10}N_2]$ ($[M+H]^+$) 732.1794, Found 732.1809; Elemental Analysis calcd (%) $C_{41}H_{26}BF_{10}N_2$: C 65.69, H 3.03, N 3.83; Found: C 38.67 ,H 2.30, N 3.83. Elemental analysis was inexplicably low for carbon and hydrogen, despite HRMS(DART) demonstrating purity.

Generation of $C_{14}H_{10}(N(C_6H_3Me_2)B(C_6F_5)_2)_2$ (19). The procedure used for compound **18**, using the same quantities of reagents, was followed. Separation of **19** from compounds **17** and **18** was achieved by flash column chromatography (eluent = 95:5 pentane:DCM) and was isolated in very low yield (~ 2 %) as grains of a magenta coloured solid. ^{1}H NMR (400 MHz, $CDCl_3$, 298 K): δ 7.63 (d, $^3J_{HH}$ = 7.4 Hz, 2H, H_3/H_{12}), 7.38 (t, $^3J_{HH}$ = 7.9 Hz, 2H, H_4/H_{11}), 7.23 (t, $^3J_{HH}$ = 7.6 Hz, 2H, H_5/H_{10}), 6.98 (d, $^3J_{HH}$ = 7.7 Hz, 2H, H_6/H_9), 6.75-6.60 (br m, 4H, H_{17a} & H_{16a}), 6.47 (br s, 2H, H_{16b}), 6.16 (brs, 2H, H_{17b}), 5.34 (s, 2H, N-H), 2.10 (s, 6H, H_{19}); ^{11}B NMR (128 MHz, $CDCl_3$, 298 K): δ 36.4 (br s); $^{13}C\{^1H\}$ NMR (126 MHz, $CDCl_3$, 298 K): 140.8 (s, C_{15}), 137.3 (s, C_{18}), 135.0 (s, C_7/C_8), 131.5 (s, C_3/C_{12}), 130.4 (s, C_2/C_{13}), 129.8 (s, C_5/C_{10}), 128.9 (s, C_{17a}), 128.7 (s, C_4/C_{11}), 128.1 (s, C_{16a}), 127.6 (s, C_{16b}), 127.1 (s, C_{17b}), 122.7 (s, C_6/C_9), 66.6 (s, C_1/C_{14}), 29.9 (s, C_{19}); ^{19}F NMR (377 MHz, $CDCl_3$, 298 K): δ –128.2 (br 1F, *o*-C_6F_5), –130.3 (br 1F, *o*-C_6F_5), -131.0 (m, 1F, *o*-C_6F_5), -132.3 (m, 1F, *o*-C_6F_5), -153.4 (t, $^3J_{FF}$ = 20.3 Hz, 1F, *p*-C_6F_5), -161.0 (br s, 2F, *p*-C_6F_5), -161.8 (ddd, $^3J_{FF}$ = 22.6 Hz & 21.8 Hz, $^4J_{FF}$ = 9.1 Hz, 1F, *m*-C_6F_5), -162.0 (ddd, $^3J_{FF}$ = 22.4 Hz & 22.0 Hz, $^4J_{FF}$ = 9.4 Hz, 1F, *m*-C_6F_5), HRMS (DART) calcd for $[C_{33}H_{17}BF_{10}N]$ ($[M+H]^+$): 628.1294, Found 628.1307; MS (EI) calcd for $[C_{52}H_{24}B_2F_{20}N_2]$ ($[M]^+$): 1078.18, Found 1078.2. The major peak for compound **19** by both DART-MS and EI-MS is the fragmentation product from loss of $[N(C_6H_3Me)B(C_6F_5)_2]$.

X-ray crystallography X-ray crystallographic data were collected on a Bruker Apex2 X-ray diffractometer at 150±2 K using a graphite monochromator with MoK(α) radiation (λ = 0.71073 Å) and the Bruker APEX-2 software[54] package. Suitable crystals were selected and mounted in Paratone-N oil on a MiTeGen cryoloop, then placed in the cold (N_2) stream of the diffractometer. Unit cell parameters were determined from consecutive scans at different orientations. The data were integrated using the SAINT software package[55] and a multi-scan absorption correction was applied using SADABS[56]. All structures were solved and refined by direct methods in the SHELXTL suite of programs using XS and refinement by full-matrix least-squares on F^2 using XL.[57,58] All non-hydrogen atoms were subjected to anisotropic refinement and carbon-bound hydrogen atoms were placed in calculated positions using an appropriate riding model and coupled isotropic temperature factors (U_{iso}(H) = 1.2U_{eq}(C)). Oxygen- and nitrogen-bound hydrogen atoms were located in the difference Fourier map and were refined with restraints of the O-H (0.84(2) Å) and N-H (0.91(2) Å) bond lengths and with U_{iso}(H) = 1.5U_{eq}(O).

EPR spectroscopy A Bruker ECS-EMX X-band EPR spectrometer equipped with an ER4119HS cavity was used for all electron paramagnetic resonance (EPR) measurements. Samples were measured at 298 K as dilute toluene solutions. EPR simulations were performed using PEST WinSIM Software.

Cyclic Voltammetry Electrochemistry was performed with a BASi Epsilon potentiostat and BASi RDE-2 Electrode cell stand. A three-electrode cell with a 3.0 mm diameter glassy carbon working electrode, a Ag/AgCl reference electrode, and a Pt wire counter electrode was used, collected at a 100 mV s^{-1} scan rate (unless otherwise stated). 0.5 mM sample solutions were prepared in the dry-nitrogen atmosphere of a glovebox, using dry dichloromethane solution, and measured in the presence of 0.5 mM ferrocene (Fc/Fc^+ reference standard) and 0.1 M tetrabutylammonium tetrafluoroborate electrolyte. Ferrocene (98% purity) and tetrabutylammonium tetrafluoroborate (99% purity) were obtained from Sigma Aldrich and used without any further purification.

UV-visible spectroscopy An Agilent 8453 UV-Vis spectrophotometer and 1 cm pathlength quartz cuvettes with PTFE stoppers were used to collect all UV-Vis absorption spectra. Analyte stock solutions were prepared in volumetric flasks in an inert nitrogen atmosphere glovebox, using dry dichloromethane, and were diluted accordingly.

Computational details All density functional theory (DFT) calculations were performed by employing Turbomole 7.0 software.[59] Harmonic vibrational frequency calculations were conducted at the PBEh-3c level to characterize the nature of the stationary points along the reaction coordinates: no imaginary frequencies were found for the local minima, and one and only one imaginary frequency for the transition states. The thermostatistical contributions to the free energy in the

Dalton Transactions Accepted Manuscript

This journal is © The Royal Society of Chemistry 20xx

Please do not adjust margins
View Article Online
DOI: 10.1039/C7DT01024A

Published on 28 March 2017. Downloaded by University of Newcastle on 28/03/2017 21:38:16.

gas phase were obtained from a modified rigid-rotor-harmonic oscillator approximation[60] at temperatures of 298.15 and 373.15 K, respectively, and for 1 atm pressure. The density-fitting RI-J[61,62] approach for the Coulomb integrals was used to accelerate the geometry optimization and frequencies calculations. Accurate electronic energies were obtained from single point calculations at the PW6B95 level[46] upon the optimized structures, with the BJ-damped variant of the DFT-D3 dispersion correction[44,45] in conjunction with the def2-TZVP basis set.[47,48] The COSMO-RS (Conductor-like Screening Model for Real Solvents) solvation model[49,50] was used to compute the solvation Gibbs free energies by employing the gas–phase optimized structures, and with toluene as the solvent. These calculations were done with the COSMOtherm program.[63,64] The final Gibbs free energies in solution were calculated from the gas-phase single point electronic energies plus the gas-phase thermal contributions, and the COSMO-RS solvation Gibbs free energies.

Acknowledgements

D.W.S. gratefully acknowledges the financial support from NSERC Canada and the award of Canada Research Chair. K.L.B. and L.E.L are thankful for Alexander Graham Bell Canada Graduate Scholarships and L.E.L. also gratefully acknowledges the Walter C. Sumner Foundation and Digital Specialty Chemicals for scholarships. This work was supported by the DFG in the framework of the Gottfried-Wilhelm-Leibniz prize (S.G.). The authors also thank Levy Cao for technical assistance with EPR and CV experiments, and Dr. Timothy Johnstone for help with X-ray crystallographic analyses.

Notes and references

1. P. P. Power, *Chem. Rev.*, 2003, **103**, 789−809.
2. T. Baumgartner and R. Réau, *Chem. Rev.*, 2006, **106**, 4681–4727.
3. A. Nordheider, J. D. Woollins and T. Chivers, *Chem. Rev.*, 2015, **115**, 10378-10406.
4. M. A. Shameem and A. Orthaber, *Chemistry*, 2016, **22**, 10718-10735.
5. S. M. Parke, M. P. Boone and E. Rivard, *Chem. Comm.*, 2016, **52**, 9485-9505.
6. W. Kaim and A. Schulz, *Angew. Chem. Int. Ed.*, 1984, **12**, 615-616.
7. M. A. Tehfe, S. Schweizer, A. C. Chany, C. Ysacco, J. L. Clement, D. Gigmes, F. Morlet-Savary, J. P. Fouassier, M. Neuburger, T. Tschamber, N. Blanchard and J. Lalevee, *Chemistry*, 2014, **20**, 5054-5063.
8. J. D. Hoefelmeyer and F. P. Gabbaï, *J. Am. Chem. Soc.*, 2000, **122**, 9054-9055.
9. H. Braunschweig, F. Breher, C. W. Chiu, D. Gamon, D. Nied and K. Radacki, *Angew. Chem. Int. Ed.*, 2010, **49**, 8975-8978.
10. S.-H. Ueng, A. Solovyev, X. Yuan, S. J. Geib, L. Fensterbank, E. Lacôte, M. Malacria, M. Newcomb, J. C. Walton and D. P. Curran, *J. Am. Chem. Soc.*, 2009, **131**, 11265-11262.
11. H. Braunschweig, I. Krummenacher, L. Mailander, L. Pentecost and A. Vargas, *Chem. Comm.*, 2016, **52**, 7005-7008.
12. R. Köster, G. Benedikt and H. W. Schrötter, *Angew. Chem. Int. Ed.*, 1964, **3**, 514-515.
13. Y. Aramaki, H. Omiya, M. Yamashita, K. Nakabayashi, S. Ohkoshi and K. Nozaki, *J. Am. Chem. Soc.*, 2012, **134**, 19989-19992.
14. I. L. Fedushkin, O. V. Markina, A. N. Lukoyanov, A. G. Morozov, E. V. Baranov, M. O. Maslov and S. Y. Ketkov, *J. Chem. Soc., Dalton Trans.*, 2013, **42**, 7952-7961.
15. A. Hinchliffe, F. S. Mair, E. J. McInnes, R. G. Pritchard and J. E. Warren, *J. Chem. Soc., Dalton Trans.*, 2008, DOI: 10.1039/b712911d, 222-233.
16. R. Köster and G. Benedikt, *Angew. Chem.*, 1963, **75**, 346.
17. M. Jeon and S. Y. Kim, *Polym. J.*, 2008, **40**, 409-413.
18. L. Li, M. Jeon and S. Y. Kim, *J. Mol. Catal. A: Chem.*, 2009, **303**, 110-116.
19. B. Gao, D. Zhao, X. Li, Y. Cui, R. Duan and X. Pang, *RSC Adv.*, 2015, **5**, 440-447.
20. B. Gao, X. Luo, W. Gao, L. Huang, S. M. Gao, X. Liu, Q. Wu and Y. Mu, *J. Chem. Soc., Dalton Trans.*, 2012, **41**, 2755-2763.
21. W. Zou and C. Chen, *Organometallics*, 2016, **35**, 1794-1801.
22. H. A. Jenkins, C. L. Dumaresque, D. Vidovic and J. A. C. Clyburne, *Can. J. Chem*, 2002, **80**, 1398-1403.
23. A. V. Piskunov, I. N. Mescheryakova, G. K. Fukin, V. K. Cherkasov and G. A. Abakumov, *New J. Chem.*, 2010, **34**, 1746.
24. A. V. Piskunov, A. V. Maleeva, I. N. Mescheryakova and G. K. Fukin, *Eur. J. Inorg. Chem.*, 2012, **2012**, 4318-4326.
25. N. J. Hill, I. Vargas-Baca and A. H. Cowley, *J. Chem. Soc., Dalton Trans.*, 2009, DOI: 10.1039/b815079f, 240-253.
26. J. R. Lawson, L. C. Wilkins, M. Andre, E. C. Richards, M. N. Ali, J. A. Platts and R. L. Melen, *J. Chem. Soc., Dalton Trans.*, 2016, **45**, 16177-16181.
27. L. Weber, J. Förster, H.-G. Stammler and B. Neumann, *Eur. J. Inorg. Chem.*, 2006, **2006**, 5048-5056.
28. W. W. Schoeller and S. Grigoleit, *J. Chem. Soc., Dalton Trans.*, 2002, DOI: 10.1039/b102843j, 405-409.
29. L. E. Longobardi, L. Liu, S. Grimme and D. W. Stephan, *J. Am. Chem. Soc.*, 2016, **138**, 2500-2503.
30. L. E. Longobardi, P. Zatsepin, R. Korol, L. Liu, S. Grimme and D. W. Stephan, *J. Am. Chem. Soc.*, 2017, **139,** , 426-435.
31. C. C. Chong and R. Kinjo, *ACS Catal.*, 2015, **5**, 3238-3259.
32. S. M. Mansell, C. J. Adams, G. Bramham, M. F. Haddow, W. Kaim, N. C. Norman, J. E. McGrady, C. A. Russell and S. J. Udeen, *Chem. Commun.*, 2010, **46**, 5070-5072.
33. V. J. Richards, A. L. Gower, J. E. Smith, E. S. Davies, D. Lahaye, A. G. Slater nee Phillips, W. Lewis, A. J. Blake, N. R. Champness and D. L. Kays, *Chem. Comm.*, 2012, **48**, 1751-1753.
34. Solutions of compound 4 in polar and non-polar solvents show <10 % degradation, as evidenced by the appearance of HC6F5, over the course of 14 days at ambient temperature, or 4 months at -35 ° C. In the solid state compound 4 shows no decomposition after 4 months of storage under an inert atmosphere of nitrogen.

Dalton Transactions Accepted Manuscript

Please do not adjust margins

View Article Online
DOI: 10.1039/C7DT01024A

35. D. J. Mathre, A. S. Thompson, A. W. Douglas, K. Hoogsteen, J. D. Carroll, E. G. Corley and E. J. J. Grabowski, *J. Org. Chem.*, 1993, **58**, 2880–2888.
36. K. Mahender Reddy, E. Bhimireddy, B. Thirupathi, S. Breitler, S. Yu and E. J. Corey, *J. Am. Chem. Soc.*, 2016, **138**, 2443-2453.
37. A.-M. Fuller, D. L. Hughes, S. J. Lancaster and C. M. White, *Organometallics*, 2010, **29**, 2194-2197.
38. R. J. Doerksen and A. J. Thakkar, *J. Phys. Chem. A*, 1999, **103**, 2141-2151.
39. L. Erdey and R. C. Pink, *Talanta*, 1962, **9**, 329-332.
40. K. Kano, M. Nakagawa, K. Takagi and T. Ikeda, *J. Chem. Soc., Perkin Trans. 2*, 1997, 1111-1120.
41. S. M. Carter, A. Sia, M. J. Shaw and A. F. Heyduk, *J. Am. Chem. Soc.*, 2008, **130**, 5838-5839.
42. F. Calderazzo, C. Forte, F. Marchetti, G. Pampaloni and L. Pieretti, *Helv. Chim. Acta*, 2004, **87**, 781-789.
43. S. Grimme, J. G. Brandenburg, C. Bannwarth and A. Hansen, *J. Chem. Phys.*, 2015, **143**, 054107.
44. S. Grimme, J. Antony, S. Ehrlich and H. Krieg, *J. Chem. Phys.*, 2010, **132**, 154104.
45. S. Grimme, S. Ehrlich and L. Goerigk, *J. Comput. Chem.*, 2011, **32**, 1456-1465.
46. Y. Zhao and D. G. Truhlar, *Journal of Chemical Physics A*, 2005, **109**, 5656–5667.
47. F. Weigend and R. Ahlrichs, *Phys. Chem. Chem. Phys.*, 2005, **7**, 3297-3305.
48. F. Weigend, *Phys. Chem. Chem. Phys.*, 2006, **8**, 1057-1065.
49. A. Klamt and G. Schüürmann, 1993, 799-805.
50. A. Klamt, *Journal of Chemical Physics A*, 1995, **99**, 2224–2235.
51. G. A. Abakumov, V. K. Cherkasov, N. O. Druzhkov, Y. A. Kurskii, G. K. Fukin, L. G. Abakumova and T. N. Kocherova, *Synth. Commun.*, 2006, **36**, 3241-3247.
52. V. K. Cherkasov, N. O. Druzhkov, T. N. Kocherova, A. S. Shavyrin and G. K. Fukin, *Tetrahedron*, 2012, **68**, 1422-1426.
53. D. J. Parks, W. E. Piers and G. P. A. Yap, *Organometallics*, 1998, **7**, 5492-5503.
54. Bruker-AXS, *APEX2*, Madison, Wisconsin, USA, 2014.
55. Bruker Analytical X-ray Systems, SAINT, *Software for the CCD Detector System*, Madison, Wisconsin, USA, 1998.
56. R. H. Blessing, SADABS, *Program for absorption corrections using Siemens CCD based on the method of Robert Blessing*, *Acta Cryst.*, 1995, **A51**, 33-38.
57. G. M. Sheldrick, SHELXS-97, *Program for Crystal Structure Refinement*, University of Göttingen: Göttingen, Germany, 1997.
58. G. M. Sheldrick, SHELXL-97, *Program for Crystal Structure Refinement*, University of Göttingen: Göttingen, Germany, 1997.
59. F. Furche, R. Ahlrichs, C. Hättig, W. Klopper, M. Sierka and F. Weigend, *WIREs Comput, Mol. Sci.*, 2014, **4**, 91-100.
60. S. Grimme, *Chemistry*, 2012, **18**, 9955-9964.
61. K. Eichkorn, O. Treutler, H. Öhm, M. Häser and R. Ahlrichs, *Chemical Physics Letters*, 1995, **240**, 283-290.
62. K. Eichkorn, F. Weigend, O. Treutler and R. Ahlrichs, *Theor. Chem. Acc.*, 1997, **97**, 119–124.
63. F. Eckert and A. Klamt, COSMOtherm, *Release 14.01*, Version C3.0, COSMOlogic GmbH & Co. KG, Leverkusen, Germany, 2014.
64. F. Eckert and A. Klamt, *AIChE Journal*, 2002, **48**, 369–385.

Published on 28 March 2017. Downloaded by University of Newcastle on 28/03/2017 21:38:16.

Dalton Transactions Accepted Manuscript

This journal is © The Royal Society of Chemistry 20xx

View Article Online
DOI: 10.1039/C7DT01024A

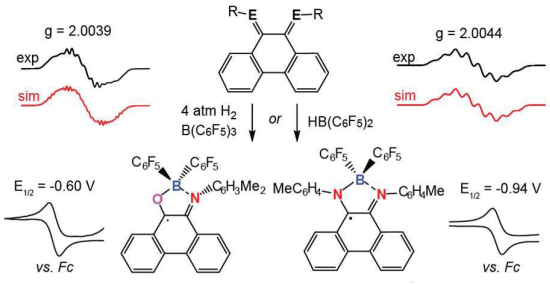

Published on 28 March 2017. Downloaded by University of Newcastle on 28/03/2017 21:38:16.

Dalton Transactions Accepted Manuscript

Please do not adjust margins